JOURNAL OF PROPULSION AND POWER
Vol. 16, No. 5, September–October 2000

Role of Oxygen-Enriched Atomization in Kerosene Spray Flames

A. K. Gupta* and T. Damm†
University of Maryland, College Park, Maryland 20742
and
S. R. Charagundla‡ and C. Presser§
National Institute of Standards and Technology, Gaithersburg, Maryland 20899

The effect of oxygen enrichment to the atomization air is examined here in a twin-fluid atomizer. A commercially available solid-cone, air-assist atomizer was used in which the atomization airstream was enriched to contain a volume fraction of 35 and 45% oxygen in nitrogen. The results are compared with the baseline case of 21% O_2 because air is the most commonly used mode of operation for twin-fluid atomizers. Data were obtained on droplet size, number density, and velocity at several spatial locations in the spray flames using a two-component phase Doppler interferometer. The global features of the spray flames, recorded photographically, were affected dramatically by oxygen enrichment of the atomization air. Specifically, the flame luminosity increases, and the flame height and volume decreases with an increase in oxygen concentration supplied to the atomization air. A moderate increase in oxygen concentration produced a whitish color high-temperature violent combustion zone near the nozzle exit. In addition, flames with oxygen-enriched atomization air reduced the number of unburned droplets escaping the flame plume into the surrounding environment. This observation was supported by the phase Doppler measurements in which droplet mean size and velocity increased and droplet number density decreased as a result of enhanced droplet vaporization. The results suggest that oxygen enrichment of the atomization air provides a significant improvement to the initial mixing between the reactants immediately downstream of the nozzle exit. This improvement, in turn, influences droplet vaporization and transport, flame stability, and combustion intensity.

Introduction

THE processes of liquid-fuel atomization, mixing, and evaporation are of fundamental importance to the efficient operation of all liquid-fueled combustion devices. Liquid fuels are atomized by imparting some instability to the fuel flow at the nozzle exit. Whatever the type of fuel atomizer (pressure-jet or twin-fluid), the objective is to achieve a large surface-area-to-volume ratio of the liquid so that the subsequent smaller droplet sizes enhance fuel vaporization and yield highly efficient combustion. The droplet size, as well as the gas composition surrounding the droplet, is of special importance because these parameters directly affect the ignition energy required for the droplet to vaporize and burn. Thus, spray quality, as governed by the type of injector employed for atomization, affects all of the processes involved in the combustion of the fuel. One injector design that has been employed over the years, in place of the commonly used pressure-type nozzles, to enhance spray quality is the twin-fluid atomizer (e.g., air-assist or air-blast types).[1–3] Air-assist atomizers are essentially pressure-swirl nozzles that use a fairly low airflow rate at high velocity to enhance atomization at low fuel pressures. The atomization airflow rate is typically less than 10% of the total air supplied to the burner. In contrast, air-blast atomizers use large airflow rates at moderate air velocity. These atomizers use air as the fluid for atomization of the liquid fuel. In addition to improved atomization, injection of air directly into the spray (as opposed to diffusion from the surrounding combustion air) enhances the availability of oxidant to the fuel for combustion.

One concept to further enhance the benefits of air-assisted atomization is to enrich the combustion airstream with oxygen. Oxygen-enriched combustion has been used in several industrial furnace systems.[4,5] In these applications the burner combustion air is blended with pure oxygen so as to enrich the availability of oxygen during combustion. The degree to which oxygen replaces air can vary between air only (volume fraction of 21%) and pure oxygen. The use of oxygen-enriched combustion air can have several advantages such as increased droplet vaporization, combustion kinetics, flame stability, gas temperature, and luminosity (i.e., heat transfer), and reduced hazardous emissions.[1,2] Increased oxygen concentration also reduces the available nitrogen in the air. Nitrogen acts as a diluent and increases the gas volume that passes through the combustion chamber for a given amount of fuel. Nitrogen in air also acts as an energy sink that carries heat away through the stack. The flame gas temperature increases significantly when combustion air is enriched with oxygen. The calculated adiabatic flame temperature for natural gas increases from 2199 K to more than 3033 K when air is replaced with oxygen. In most combustion systems the dominant mode of heat transfer from the flame is via radiation. Because the relationship of radiation heat transfer to the absolute temperature is quartic (fourth power), the higher temperature associated with oxygen increases the heat transfer to the thermal load (e.g., for thermal treatment of materials or steam generation), which, in turn, increases the processing rate. This means that more of the material can be processed in an existing system or that new systems can be made smaller while accomplishing the same processing rate.[6]

The possibilities of a highly productive and compact furnace become apparent when the amount of heat loss to the combustion products is reduced significantly; the flue gas volume in oxygen/fuel combustion systems is less than one-third of that in air/fuel systems. In addition, oxygen/fuel systems require smaller gas transfer, exhaust, and pollution control equipment because of less volume of gas with oxygen as compared to air. This benefit has been used with incinerators that process a variety of wastes and materials.[4,5] However, the need and costs required to supply large quantities of oxygen are of concern. The supply of oxygen for enrichment of the combustion air can be provided from air separation plants that use membrane technologies to partly remove nitrogen from the air. The expectation is that costs would drop as demand increases.[6]

Received 18 August 1998; revision received 6 April 1999; accepted for publication 6 August 1999.

*Professor, Department of Mechanical Engineering. Fellow AIAA.
†Graduate Student, Department of Mechanical Engineering.
‡Research Engineer, Thermal and Reactive Processes, Process Measurements Division, Chemical Science and Technology Laboratory.
§Leader, Thermal and Reactive Processes, Process Measurements Division, Chemical Science and Technology Laboratory. Associate Fellow AIAA.

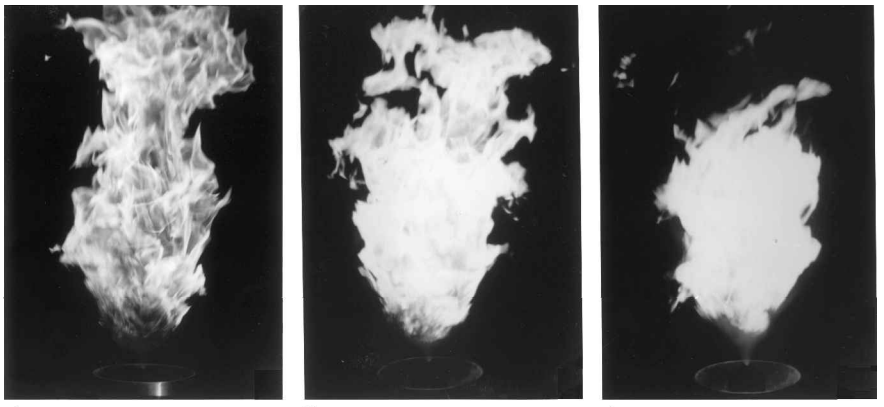

Fig. 1 Observed features of the spray flame for varying oxygen enrichment of the atomization air: a) 21% O_2 (baseline air), b) 35% O_2, and c) 45% O_2.

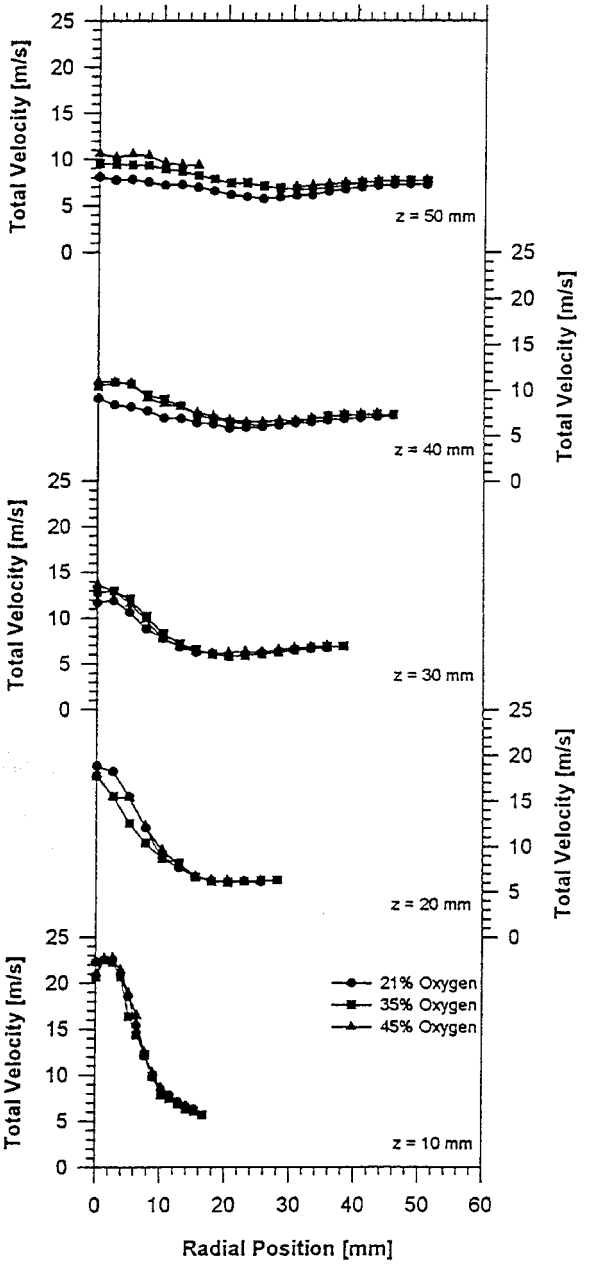

Fig. 2 Variation of the droplet total velocity with radial and axial positions for different oxygen concentrations of the atomization air.

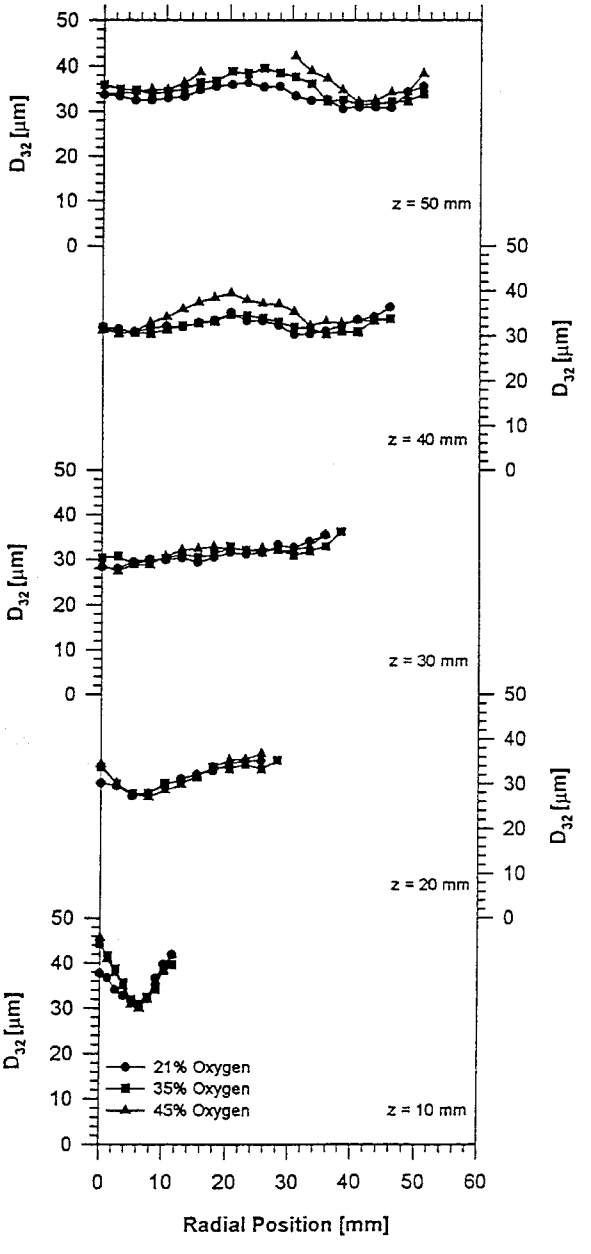

Fig. 3 Variation of the droplet Sauter mean diameter (D_{32}) with radial and axial positions for different oxygen concentrations of the atomization air.

Injection of oxygen-enriched air via the atomization airstream, as opposed to the commonly used approach through the combustion air passage, strategically provides additional oxidant to the near-field fuel-rich regions of the spray.[7] At present there is scant information on the role of oxygen-enriched atomization air on droplet transport and flame characteristics. Thus, the objective of this investigation was to examine the effect of oxygen-enriched atomization air in an air-assist atomizer on flame structure and droplet characteristics in swirling spray flames. The amount of oxygen in the atomization air was set at volume fractions of 21, 35, and 45%. Global features of the spray flames were recorded photographically to provide information on droplet transport, flame size, shape, luminosity, and stand-off distance from the nozzle exit. Droplet size, velocity, and number density distributions were measured using a two-component phase Doppler interferometry system. The data were collected with recommended voltage settings on the photomultiplier detectors.

Experimental Apparatus

Experiments are carried out in a spray combustion facility that is used to simulate the combustion processes in practical combustion systems. The facility consists of a swirl burner in which a cascade rotates 12 vanes simultaneously to impart the desired degree of swirl to the combustion air that surrounds the centrally located fuel nozzle. In these experiments a commercially available stainless-steel, internal mixing, air-assist nozzle was used that produced a solid-cone spray. The nozzle was operated at an atomization airflow rate of 1.51 kg/h and line pressure of 170 kPa, which formed a spray cone angle of approximately 75 deg. Data in this study were obtained for oxygen volume fractions of 21 (baseline case of air), 35, and 45%. The concentration of oxygen in the atomization air was limited to a volume fraction of 45% in order to ensure safe operation of the atomizer. The composition of the assisting gas was controlled by mixing measured amounts of oxygen with air. A chamber with a fixed bed of glass beads was used to mix the two gas streams. The volume percent of oxygen in the mixed oxygen/air gas stream was then calculated from the flow rates of the metered oxygen and total atomization gas streams. For each case the momentum flux of the atomization gas was kept the same. This mode of operation allowed the three cases to be compared independently of gas density and isolated the effects of chemistry.[8] Studies on the effect of atomization gas on pollutant concentrations[9] showed

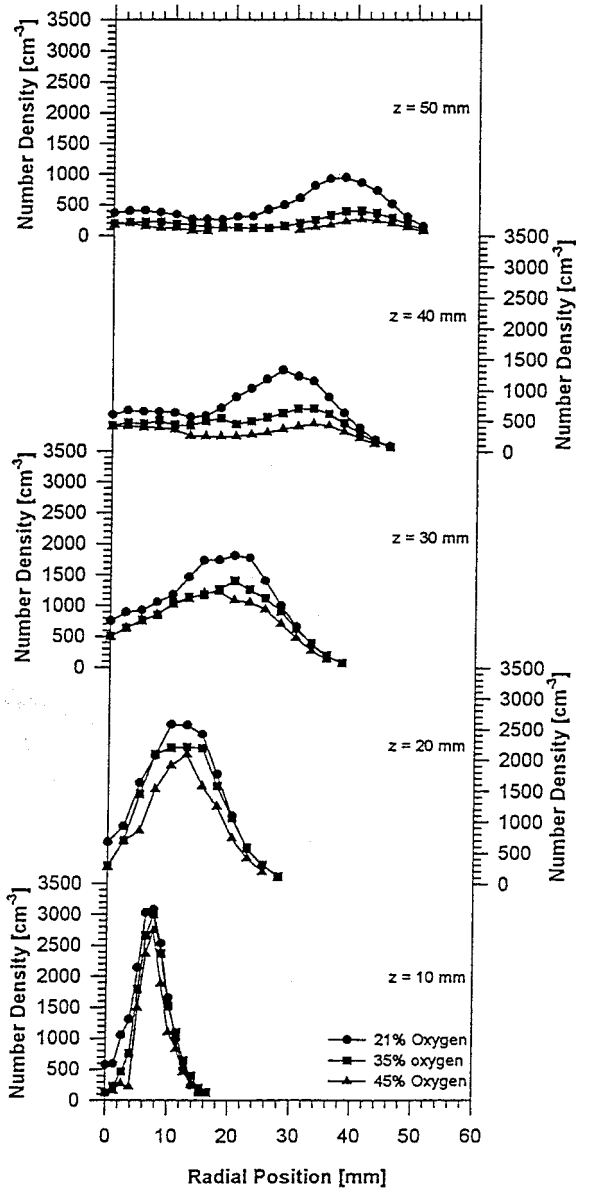

Fig. 4 Variation of the droplet number density with radial and axial positions for different oxygen concentrations of the atomization air.

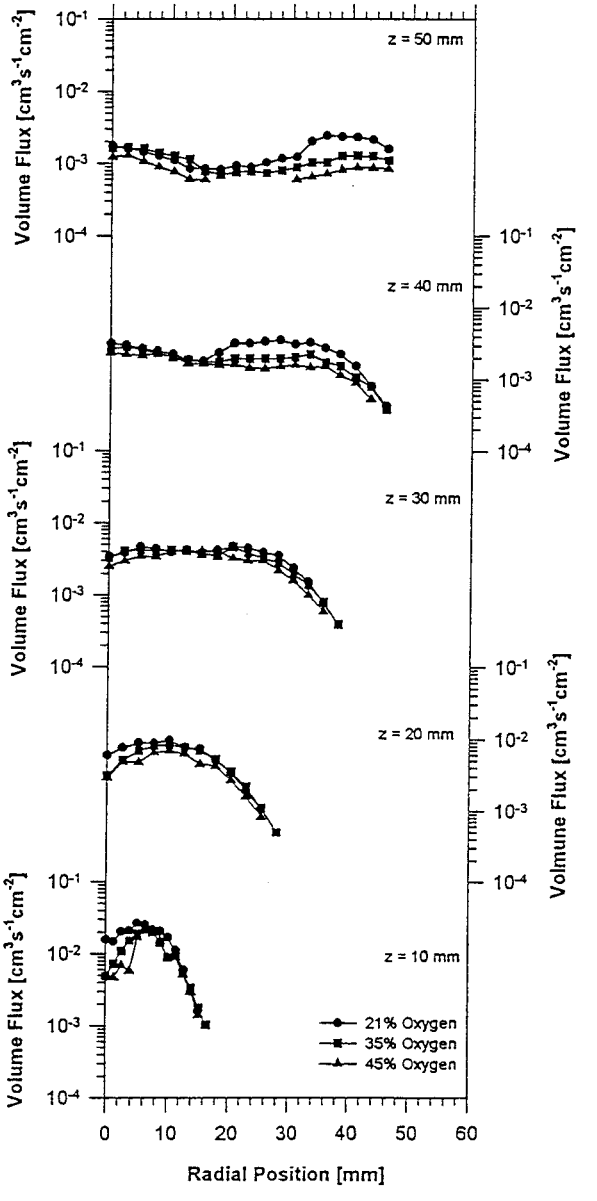

Fig. 5 Variation of the droplet volume flux with radial and axial positions for different oxygen concentrations of the atomization air.

that substituting atomization air with CO_2 resulted in significant changes to the flame structure in the near region, but the measured pollutants showed negligible differences. The global flame structure and droplet dynamics are much affected by some atomization gases.[10,11]

The combustion air that coflows about the fuel stream was air. The swirl vane angle was fixed at 32 deg, and this corresponded to a swirl number of about 0.29 (Ref. 12). This swirl number provided stable flames for the baseline and each oxygen-enriched atomization air case. In this study the total combustion air and kerosene fuel flow rates were 210 and 4.1 kg/h, respectively. The combustion air was more than two orders of magnitude greater than the atomization air. This provided an inlet equivalence ratio of approximately 0.28. Laser-sheet beam photography was used to illuminate vertical cross sections of the spray flame through the spray centerline. The spray flame features were also recorded photographically using a 35-mm camera. A 400 ASA film at wide aperture of the camera lens (for achieving small depth of field) was used at or exposure time of 1/125 s. The burner was mounted on a stepper-motor-controlled three-dimensional traversing mechanism, which allowed the burner to move independently of the optics that were fixed in position about the burner. This arrangement allowed precise alignment of the optical diagnostic equipment with the spray and enabled spatially resolved measurements in the flames. Additional details on the burner assembly are given in Refs. 8 and 13.

A two-component phase Doppler interferometer (PDI) was used to determine fuel droplet size, number density, and velocity in the swirling kerosene spray flames (see Refs. 8 and 14 for details). Measurements were carried out in the radial direction with the PDI from the spray centerline to the edge of the spray in increments of 1.27 mm at an axial position z of 10 mm downstream from the nozzle exit and increments of 2.54 mm at $z = 15$, 20, 25, 30, 35, 40, 50, and 60 mm. The data rates were determined according to the procedure discussed in Ref. 15. At every measurement point 10,000 validated samples were recorded to determine the statistical properties of the spray. In regions of the spray where the droplet arrival rate was too small because of the lack of droplets at that location, a sampling time of 2 min was used for these measurements. Data were not obtained at those locations of the spray where the data rate was almost negligible and would not provide any meaningful statistics. The instrument provided repeatable data to within 5% for droplet mean size and velocity. The repeatability of the data obtained from day to day was within this margin of error.

Results and Discussion

Observed Flame Characteristics

The global features of the spray flame were observed to be influenced dramatically by the amount of oxygen enrichment of the atomization air. Laser-sheet beam photography was used to illuminate vertical cross sections of the spray and flame through the spray longitudinal axis. The luminosity of the kerosene spray flame was high so that it was not possible to examine the droplets inside the flame. The larger droplets were observed with the laser

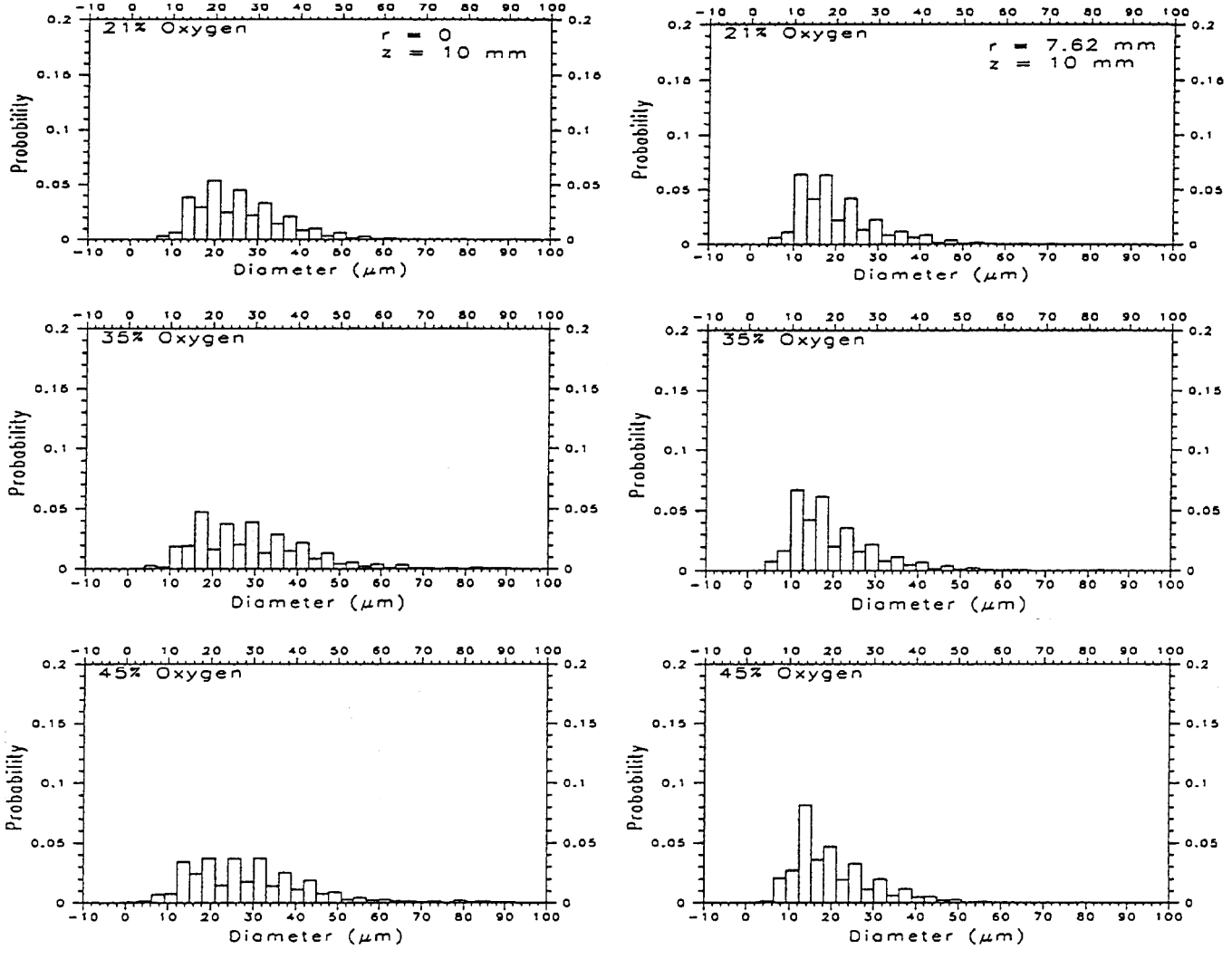

Fig. 6 Droplet size distribution at $z = 10$ mm for $r = 0$ and 7.62 mm with different oxygen concentrations of the atomization air.

sheet in the region upstream of the flame front and downstream at locations outside of the flame plume. The results showed that droplets were transported through the flame sheet ballistically and into the surrounding environment for the baseline air case; however, as the oxygen concentration increased, this feature was reduced significantly. The flame features were also recorded photographically using a 35-mm camera. A representative set of images is shown in Fig. 1, in which the oxygen concentration of the atomization air is 21 (baseline air), 35, and 45%, respectively. The stand-off distance of the flame front from the burner nozzle exit was about 15 mm with baseline air. As the oxygen concentration increased, the stand-off distance of the flame decreased slightly. The flame height and volume became smaller and more compact, respectively, with increased oxygen concentration (see Fig. 1). At very high O_2 levels there was an intense blue flame zone immediately downstream of the nozzle exit. The flame became louder at higher oxygen concentrations. The flame luminosity increased significantly at higher oxygen concentrations (compare the luminosity of Fig. 1a at 21% O_2, with Fig. 1c at 45% O_2). The increased flame luminosity suggests that the radiative heat transfer from the 45% O_2 flame (see Fig. 1c) is much higher than the baseline air case (see Fig. 1a). This suggests a change in soot concentration in the flames. Quantitative information on the soot concentration and heat flux from flames will be reported in one of our future publications. The variation in the flame features with oxygen concentration also suggests that the local upstream injection of oxygen strategically into the spray can have a dramatic influence on the entire flame structure. Unlike inert-gas injection (see Refs. 7–9), in which these atomization gases influence primarily the spray properties in the near region of the flame, injection of oxygen-enriched atomization air affects the entire flame structure. Thus, the spray characteristics for each flame should be different.

Mean Spray Characteristics

The observed flame features indicated that oxygen enrichment of the atomization air has a dramatic effect on the spray characteristics in the near-nozzle region, which, in turn, influences the entire flame structure. Therefore, the study focused on determining quantitatively how the spray characteristics (viz., the measured droplet size and velocity distributions and subsequent determination of the mean properties) under burning conditions change with oxygen concentration of the atomization gas at different spatial positions.

Typical results for droplet mean total velocity and Sauter mean diameter with respect to radial position are presented in Figs. 2 and 3, respectively, at different axial positions downstream of the nozzle exit and at oxygen volume fractions of 21, 35, and 45% for the atomization air. At upstream locations (i.e., $z = 10$ mm) the results indicate a maximum value of droplet velocity at the center of the spray. Droplet velocity decays rapidly as one progressively moves radially outward toward the edge of the spray cone and surrounding combustion air (see Fig. 2). The oxygen content of the atomization air was found to have negligible influence on droplet mean

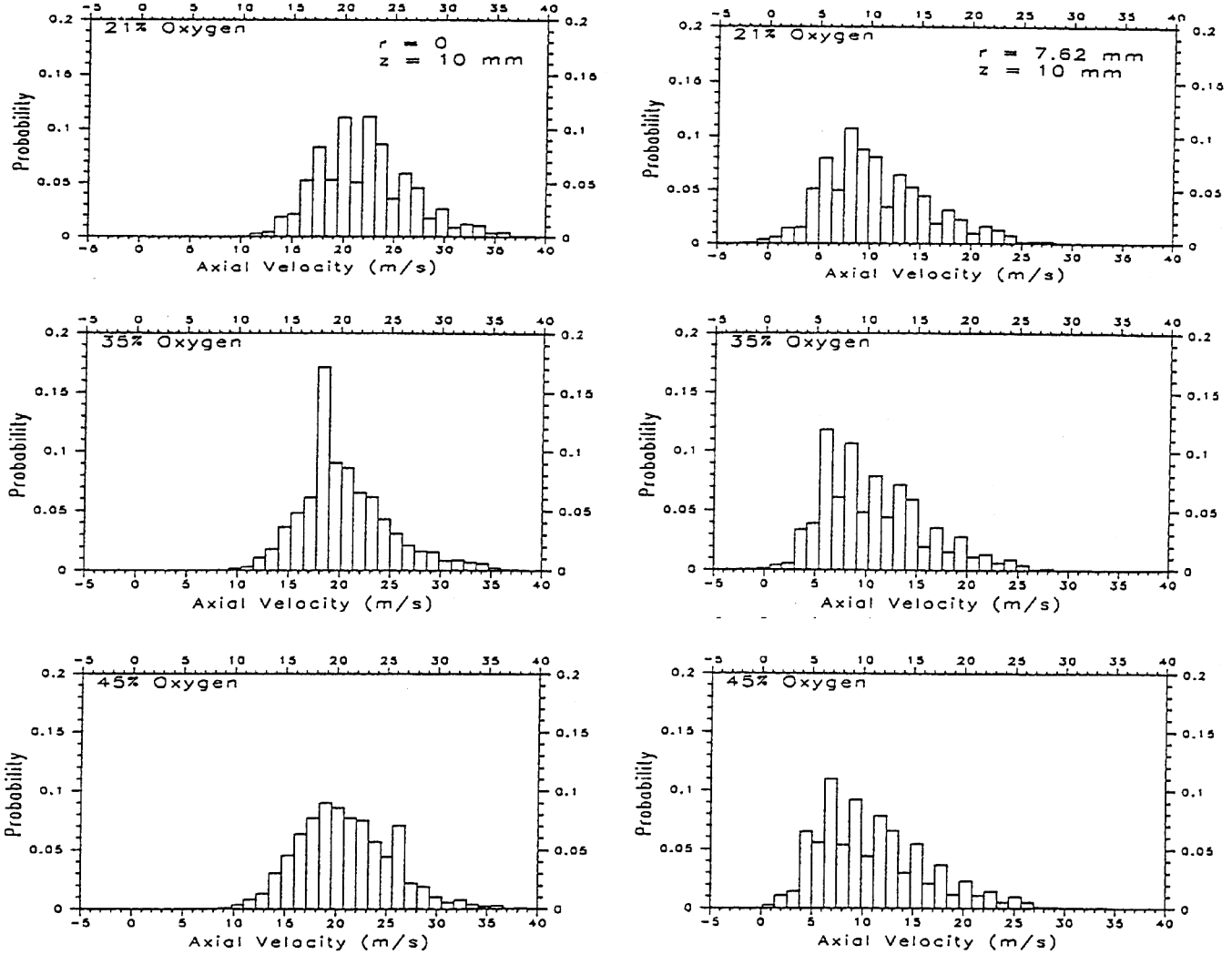

Fig. 7 Droplet axial velocity distribution at $z = 10$ mm for $r = 0$ and 7.62 mm with different oxygen concentrations of the atomization air.

velocity at this axial location, which was upstream of the flame front. This result was attributed to the similar effects of combustion on droplet transport for each flame and because of the constant momentum flux of the atomization air. The flame luminosity does, however, provide an energy feedback to the droplets, which affects the droplet vaporization and mean size, as presented in Fig. 3. The results for $z = 10$ mm indicate that there is an increase in the value of droplet Sauter mean diameter with increasing oxygen concentration of the atomization air in the central portion of the spray. This change in droplet mean size is attributed to increased droplet vaporization and depletion of the smaller size droplets.[13] Toward the edge of the spray, the mean size decreases, which corresponds to a higher concentration of droplets (compare the droplet size at the centerline to the radial position of $r = 7.62$ mm in Fig. 3). At $r > 7.62$ mm the mean size increases again as a result of droplet vaporization.

Number density with respect to radial position is presented in Fig. 4 at different axial locations for the baseline air and oxygen-enriched cases. The results indicate a decrease in droplet number density for increasing oxygen concentration of the atomization air. Increased oxygen content affected the entire cross section of the spray (and the spray flame). This may be attributed to the thermal energy feedback (including radiative) from the flame to the entire spray field emanating from the nozzle exit. The importance of radiative energy vs temperature of the flame requires substantiation and further examination. The droplet number density at $z = 10$ mm and near the spray edge, i.e., $r = 7.62$ mm, was at least an order of magnitude greater than that found in the central region of the flame. The radial position of the peaks in number density also appear to correspond to minima in the Sauter mean diameter (compare Figs. 3 and 4). Note that the peak value of droplet number density is at an off-axis radial position for axial locations near the nozzle exit (e.g., $z = 10$ mm) even though the nozzle is characterized as producing a solid-cone spray. This result is attributed, in part, to the presence of the toroidal recirculation zone, which helps to divert the droplet stream radially outward from the central region of the flame. The solid-cone nature of the spray is still apparent because droplets are detected near the center of the spray, whereas detection of droplets in this region would be negligible for a hollow-cone spray, especially at positions further downstream. Further support is provided in Fig. 5 by the variation of droplet volume flux (i.e., droplet volume per unit time per unit measurement cross-sectional area) with radial position at different axial locations. These results also indicate the presence of a considerable volume of droplets near the center of the spray.

Further downstream from the nozzle exit at any position within the flame, the differences between the baseline air and oxygen-enriched cases become more pronounced because of the influence of the initial ignition and vaporization processes on droplet burning. The droplet mean total velocity and Sauter mean diameter at $z = 50$ mm (see Figs. 2 and 3, respectively) both increase, and number density (see Fig. 4) decreases as a consequence of enhancing the oxygen concentration of the atomization air. The higher droplet number densities for the baseline air case, as compared to the 45% O_2 case, at $z = 50$ mm is attributed to lower temperature of the flame so that many droplets still remain at this location. Toward the edge of the spray, data are not presented at $z = 50$ mm for the 45% O_2 case because of the lack of droplets (i.e., signal) in this region. Higher gas temperatures and flame luminosity enhance droplet vaporization and reduce significantly the droplet population in this region. Indeed, when the probe volume location was moved further downstream to $z = 60$ mm (data not shown), a significant reduction in the data rate was observed such that data could not be obtained over an even larger radial distance. Outside of the flame sheet, i.e., at $r > 30$ mm and $z = 50$ mm, the data rate increased again so as to acquire data for droplet mean size, number density, and velocity. The resulting off-axis peaks for number density and volume flux (see $r > 30$ mm and $z = 50$ mm in Figs. 4 and 5) support the aforementioned observations, via laser sheet beam photography, that droplets penetrate through the flame sheet and into the surrounding environment. The droplet number density and volume flux at $r > 30$ mm and $z = 50$ mm also diminish significantly with increasing oxygen concentration. This effect appears to assist in reducing droplet transport through the flame sheet and enhancing the spray uniformity.

Droplet Size/Velocity Distributions and Arrival Times

Droplet size and velocity distributions and the time of arrival of droplets into the measurement volume of the phase Doppler system were examined at different spatial positions and compared for the baseline and two oxygen-enriched flames. The size distributions for each case are presented in Fig. 6 at $z = 10$ mm for $r = 0$ and 7.62 mm. The distributions indicate that the change in the droplet mean size for each case is attributed to the significant vaporization and reduction in number of the smaller-size droplets so that the skewness of the relative distributions is changed slightly toward the larger-size droplets as O_2 content in air increases. The size distributions (for all three cases) at the centerline are also wider than near the edge of the spray (i.e., at $z = 10$ mm and $r = 7.62$ mm). For example, the skewness of the histograms at $z = 10$ mm and $r = 0$ is 1.46 for 21% O_2 and 1.28 for 45% O_2 (a smaller positive value for skewness indicates a shift in the distribution peak toward larger droplet sizes).[12] Thus, this shift in size distribution results in a larger droplet mean size as the oxygen concentration increases.

Axial velocity distributions are presented in Fig. 7 at $z = 10$ mm, for $r = 0$ and 7.62 mm. These data support the just-mentioned results for the size distributions, namely, much higher droplet velocities are found near the spray centerline. The range of droplet axial

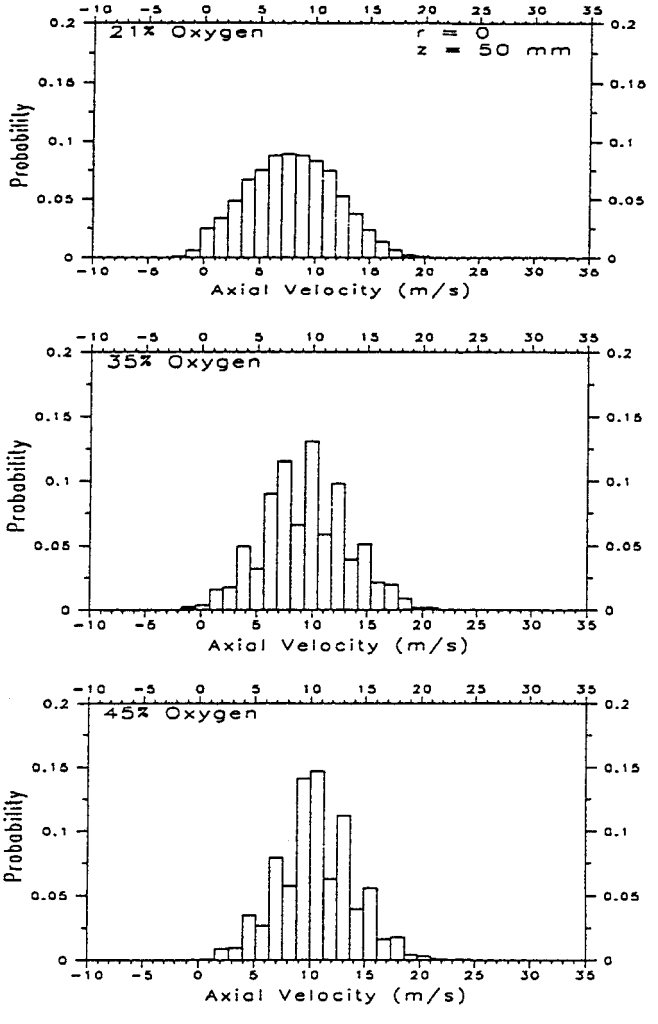

Fig. 8 Droplet axial velocity distribution at $z = 50$ mm and $r = 0$ with different oxygen concentrations of the atomization air.

velocities near the spray centerline are between 9 and 38 m/s. Near the edge of the spray, the droplet velocities are reduced significantly and range from 28 m/s to less than zero (see Fig. 7). In fact, small negative values of the axial velocity (corresponding to recirculated smaller droplets in a small vortex near the edge of the spray) are present for the baseline air case and not present in the 45% oxygen-enriched case. The arrival time sequence (data not shown) for each case indicates that recirculated droplets are detected infrequently and that the tendency is reduced with increasing oxygen concentration. The droplet axial velocity distributions at $z = 50$ mm and $r = 0$ are presented in Fig. 8. The presence of negative axial velocities found for the baseline air case are not observed for the other two oxygen-enriched cases. These results indicate that smaller droplets are redirected upstream by the larger toroidal recirculation zone that is established by the swirling combustion air. As atomization-air oxygen concentration and flame gas temperatures increase, droplets are no longer entrained by the weakened recirculation zone.

The droplet arrival time sequences for the baseline air and oxygen-enriched cases were found to have about the same data rates at the spray boundary at 10 mm downstream from the nozzle exit, see Fig. 9 at $r = 7.62$ mm. However at the center of the flame at $r = 0$ mm significant differences between the baseline case and the oxygen-enriched atomization case can be seen. The recirculated high-temperature gases associated with the oxygen-enriched case reduces the number of droplets present at the centerline, see Fig. 9 at $r = 10$ and 0 mm. However at $z = 50$ mm the droplet arrival time sequences were found to be significantly different between the baseline air and the oxygen-enriched cases at both the centerline and the spray boundary. The results presented in Fig. 10 at $z = 50$ mm and $r = 0$ (i.e., spray centerline) and $r = 38.1$ mm (i.e., near the edge of the spray) indicate clearly a reduction in the droplet population with increased oxygen enrichment at each position. The droplets are size coded in Figs. 9 and 10 so that larger diameter circles represent larger droplet sizes. The results again indicate that recirculated droplets (having negative axial velocities) are detected infrequently near the center of the spray at $z = 50$ mm (in contrast to the results obtained at $z = 10$ mm where recirculated droplets were found toward the edge of the spray). Increased oxygen concentration resulted in the elimination of droplet recirculation. Determination of the droplet trajectory angle (data not shown) also indicates that the spray is essentially axial near the spray centerline regardless of the oxygen concentration and moves radially outward at positions near the edge of the spray (except for the recirculated droplets). The shape of the droplet size distributions at $z = 50$ mm for the three cases (data not shown) remain relatively unchanged (even though the mean values change). Thus, there is no indication of preferential apportionment of the droplet sizes or any significant departure in droplet combustion behavior with oxygen enrichment to the atomization air.

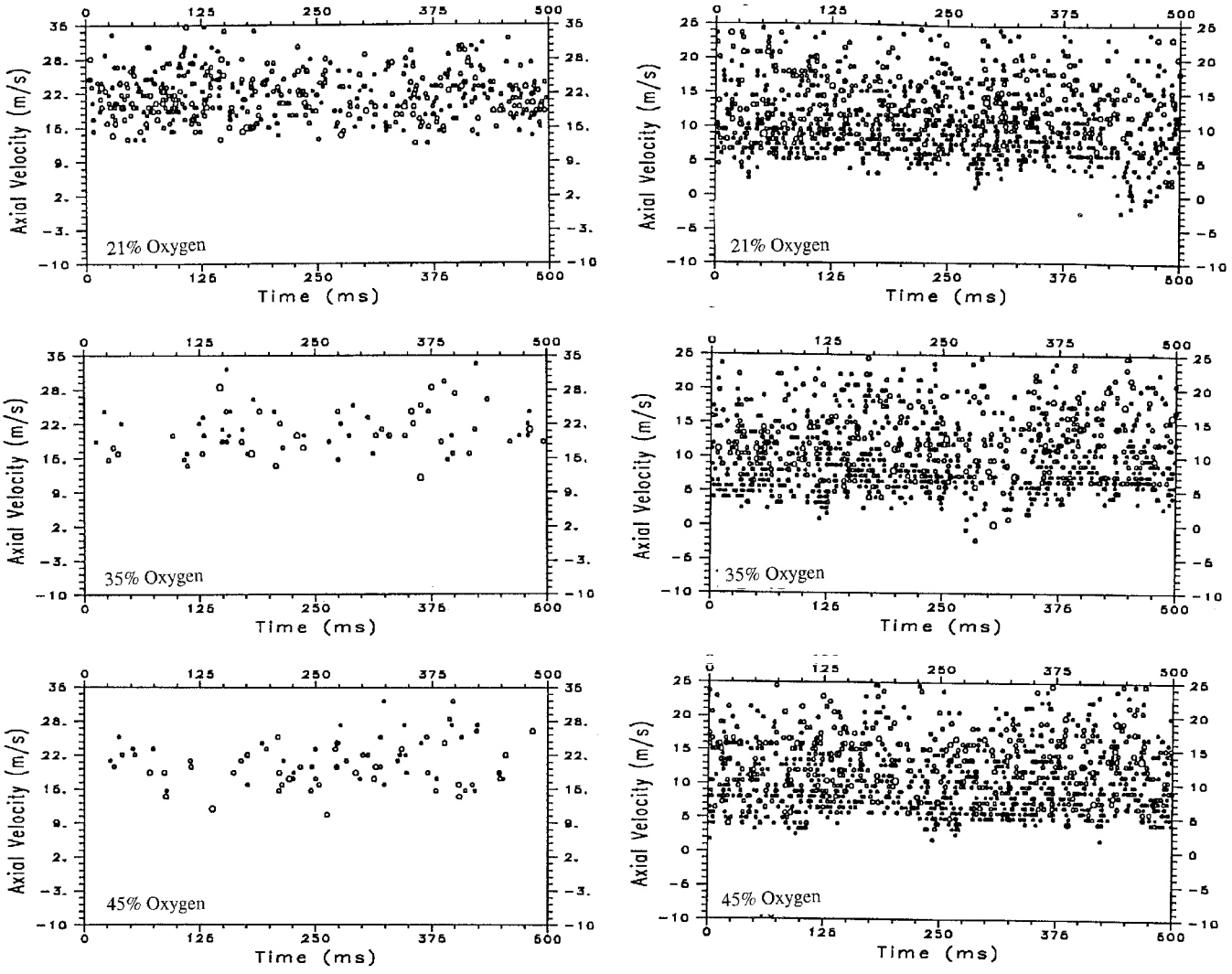

Fig. 9 Time-of-arrival sequence for droplet axial velocity at z = 10 mm for r = 0 (left column) and 7.62 mm (right column) with different oxygen concentrations of the atomization air.

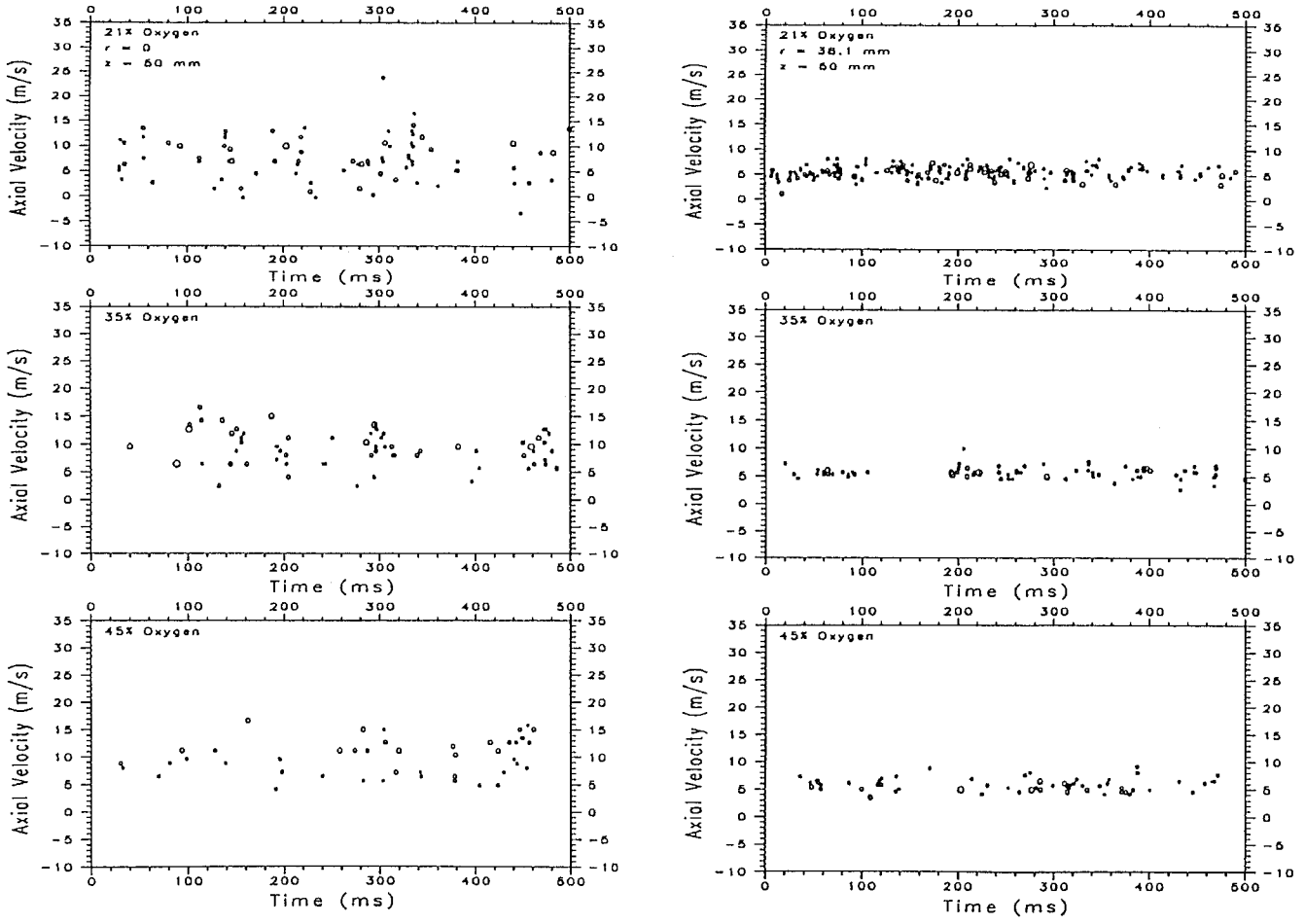

Fig. 10 Time-of-arrival sequence for droplet axial velocity at $z = 50$ mm for $r = 0$ (left column) and 38.1 mm (right column) with different oxygen concentrations of the atomization air.

Conclusions

Droplet size and velocity measurements were carried out using a commercially available air-assist atomizer with oxygen enrichment of the atomization air. Direct flame photography in conjunction with a laser-sheet beam was used to record the features of the kerosene spray flames. Flame length is reduced with oxygen enrichment to the atomization air. Droplet size and velocity distributions were obtained using a two-component phase Doppler interferometer. Droplet size, velocity, and number density were found to change significantly with increased oxygen concentration of the atomization air as a result of enhanced droplet vaporization. The results indicated that oxygen enrichment has a pronounced effect on the flame length, volume, and luminosity. The increase in flame luminosity is attributed to the initial mixing of oxygen with fuel droplets and enhanced droplet vaporization immediately downstream of the nozzle exit, which is expected to have an important effect on the flame chemistry, thermal signature, and emission levels. Introduction of a small amount of oxygen to the atomization air is shown to have a more dramatic effect on the combustion process than is achieved by introducing the same oxygen into the combustion air.

Acknowledgments

The authors wish to acknowledge the partial support of this work by the Office of Naval Research; the project scientific officer is Gabriel Roy. Technical assistance provided by Boyd Shomaker and Jim Allen is much appreciated.

References

[1]Lefebvre, A. H., *Atomization and Sprays*, Hemisphere, New York, 1989.

[2]Lefebvre, A. H., *Gas Turbine Combustion*, Hemisphere, New York, 1983.

[3]Presser, C., Gupta, A. K., and Semerjian, H. G., "Dynamics of Pressure-Jet and Air-Assist Nozzle Sprays: Aerodynamic Effects," AIAA Paper 88-3139, 1988.

[4]Fujisaki, W., and Nakamura, T., "Thermal and NO, Characteristics of High Performance Oxy-Fuel Flames," American Flame Research Committee, Sept. 1996.

[5]Murakami, H., Fujioka, M., Hase, M., Saito, T., and Hayashi, J., "Development of Oxygen/COG System for Steel Reheating," American Flame Research Committee, Sept. 1996.

[6]Hedley, J. T., Pourkashanian, M., Williams, A., and Yap, L. T., "NO, Formation in Large-Scale Oxy-Fuel Flames," *Combustion Science and Technology*, Vol. 108, 1995, pp. 311–322.

[7]*North American Combustion Handbook*, 3rd ed., North American Manufacturing Co., Cleveland, OH, 1986.

[8]Aftel, R., Gupta, A. K., Cook, C., and Presser, C., "Gas Property Effects on Droplet Atomization and Combustion in an 'Air-Assist' Atomizer," *26th Symposium (International) on Combustion*, The Combustion Inst., 1996, pp. 1645–1651.

[9]Siddiqui, N., Zhang, Z., and Gollahalli, S. R., "Effects of Atomization Gas on Some Pollutant Concentrations in a Burning Liquid Spray," *Combustion Science and Technology*, Vol. 34, 1984, pp. 105–112.

[10]Gupta, A. K., Cook, C., and Presser, C., "Effect of Atomizing Gas Properties on Droplet Dispersion in an Air-Assist Atomizer," International Conference on Liquid Atomization and Spray Systems (ICLASS), Aug. 1997.

[11]Gupta, A. K., Megerle, M., Charagundla, S. R., and Presser, C., "Spray Flame Characteristics for High Temperature Gas-Assisted Atomization," Institute of Liquid Atomization and Spray Systems (ILASS) Conf., May 1998.

[12]Gupta, A. K., Lilley, D. G., and Syred, N., *Swirl Flows*, Abacus Press, Kent, 1984.

[13]Presser, C., Gupta, A. K., and Semerjian, H. G., "Aerodynamic Characteristics of Swirling Spray Flames," *Combustion and Flame*, Vol. 92, No. 1/2, 1993, pp. 25–44.

[14]Gupta, A. K., Presser, C., Hodges, J. T., and Avedisian, C. T., "Role of Combustion on Droplet Transport in Pressure-Atomized Spray Flames," *Journal of Propulsion and Power*, Vol. 12, No. 3, 1996, pp. 543–553.

[15]Presser, C., Gupta, A. K., Semerjian, H. G., and Avedisian, C. T., "Droplet Transport in a Swirl-Stabilized Spray Flame," *Journal of Propulsion and Power*, Vol. 10, No. 5, 1994, pp. 631–638.